Acta Cryst. (1957). **10**, 1

The Crystal Structure of the *P* Phase, Mo–Ni–Cr. II. Refinement of Parameters and Discussion of Atomic Coordination*

BY DAVID P. SHOEMAKER, CLARA BRINK SHOEMAKER AND FRANK C. WILSON

Department of Chemistry, Massachusetts Institute of Technology, Cambridge 39, *Massachusetts, U.S.A.*

(*Received* 9 *May* 1956)

The crystal structure of the *P* phase, Mo–Ni–Cr, in atom ratio 42:40:18, was described in its basic features in a previous communication. The present communication describes the refinement of the lattice constants with powder photographic data and of the positional parameters and atomic scattering parameters (approximately proportional to atomic numbers) by use of generalized Fourier projections with (*hk*0) and (*hk*2) single-crystal data. The structure is primitive orthorhombic, with lattice constants $a_0 = 9{\cdot}070$, $b_0 = 16{\cdot}983$, $c_0 = 4{\cdot}752$ Å, space group D_{2h}^{16}–*Pbnm*. The unit cell contains 56 atoms in an arrangement resembling two differently oriented σ-phase unit cells in juxtaposition. The atoms have characteristic coordination polyhedra with 12, 14, 15, and 16 vertices, of which only the last does not occur in the σ phase, but does occur in α-manganese. By least squares, values were found for eight different radii, chosen in accord with the symmetry of these polyhedra, and, by summing appropriate pairs of these radii, calculated values of the 58 different interatomic distances were obtained which agreed with the observed distances with a mean deviation of 0·035 Å. A re-examination of the σ-phase distances along these lines gave closely similar results. On the basis of the radii obtained, ligands in the *P* and σ phases seem to divide distinctly into two types: a small proportion of strong, probably relatively localized, bonds, presumably of high *d* character; and many more weaker, probably more delocalized and more typically metallic, ligands. The values obtained for the scattering parameters in the *P* phase are rough, but suggest that the content of molybdenum in the atomic sites increases with coordination from approximately zero for coordination 12 to approximately 100% for coordination 16.

Introduction

The determination of the structure of the *P* phase in the molybdenum–nickel–chromium system was undertaken as a part of a program concerned with the investigation of the structures of some members of a group of binary and ternary alloys of transition metals, discovered largely by Beck and coworkers (Rideout, Manly, Kamen, Lement & Beck, 1951), and shown by them to be interrelated in their phase behavior and probably to be electron compounds related to the σ phase. This group of compounds contains, besides the *P* phase in the Mo–Ni–Cr system (Rideout *et al.*, 1951) and in the Mo–Ni–Fe system (Das, Rideout & Beck, 1952), also the δ phase in Mo–Ni (Ellinger, 1942), the *R* and *D* phases in Mo–Co–Cr (Rideout *et al.*, 1951), the μ phase in Mo–Co and other systems, and the χ phase (α-Mn structure) in Mo–Fe–Cr (Andrews, 1949). The crystal structure of the σ phase in some binary systems has been described (Shoemaker & Bergman, 1950; Bergman & Shoemaker, 1954; Dickens, Douglas & Taylor, 1951; Kasper, Decker & Belanger, 1951; Kasper & Waterstrat, 1956) and is essentially identical to the β-uranium structure (Tucker, 1950; Tucker & Senio, 1953). The crystal structures of the μ phase (Arnfelt & Westgren, 1935) and of α-manganese and the χ phase (Bradley & Thewlis, 1927; Kasper, 1954) have also been determined, and those of the δ phase (Shoemaker, Shoemaker & Fox, work in progress) and of the *R* phase (Komura, Shoemaker & Shoemaker, work in progress) have been partially determined. The structures of the μ and χ phases show strong similarities with the σ-phase structure, and there are strong indications of such similarities in the structures of the δ and *R* phases.

On the Mo–Ni–Cr phase diagram at 1200° C. the *P* phase, with atom ratio in the neighborhood of 42:40:18, lies between a σ phase around 27:27:45 and a δ phase around 50:50:0. In the Mo–Ni–Fe system a *P* phase lies between a μ phase and the same Mo–Ni δ phase.

A specimen of the *P* phase of Mo–Ni–Cr in stated weight ratio 55:32:13, corresponding to atomic ratio 42:40:18, annealed at 1200° C., was made available to us in 1951 through the kindness of Prof. Paul A. Beck, then of Notre Dame University, now of the University of Illinois. In a previous communication (Brink & Shoemaker, 1955) the basic features of the structure were reported (primitive orthorhombic, $a_0 = 9{\cdot}07$, $b_0 = 17{\cdot}01$, $c_0 = 4{\cdot}74$ Å, probable space group D_{2h}^{16}–*Pbnm*, 56 atoms in an arrangement suggestive of two differently oriented σ-phase unit cells

* Sponsored by Office of Ordnance Research.

in juxtaposition). In the present communication, refinements of the lattice constants by powder photography and of the atomic positional parameters and approximate atomic numbers by generalized Fourier projections are described, and certain features of the structure are discussed.

Table 1. *Powder photographic data for P phase*, Mo–Ni–Cr

(Ni-filtered Cu Kx radiation)

hkl	$1/d_{cal.}$ (Å^{-1})	$mF^{2*}/100$	Powder diagram $1/d_{obs.}$ (Å^{-1})	*I*
021	0·2412	8	0·2441	*vw*
121	0·2652	11	—	—
—	—	—	0·2785	*vw*†
150	0·3144	13	0·3182	*f*
221	0·3268	16	—	—
250	0·3678	16	—	—
160	0·3701	26	0·3697	*vw*
330	0·3750	18	—	—
151	0·3783	105	0·3786	*m*(*b*)
301	0·3920	58	0·3923	*w*
311	0·3864	23	—	—
340	0·4060	39	0·4067	*w*
061	0·4112	14	—	—
002	0·4209	617	0·4212	*s*
161	0·4257	179	0·4266	*ms*
170	0·4267	167		
331	0·4300	204	0·4309	*ms*
112	0·4391	20	0·4387	*vw*
350	0·4428	79	0·4440	*w*
410	0·4449	45		
420	0·4564	811	0·4569	*vs*
341	0·4573	75		
132	0·4696	127	0·4701	*w*
080	0·4710	54		
202	0·4752	139	0·4765	*vs*
171	0·4757	798		
212	0·4788	510	0·4796	*m*
042	0·4823	207	0·4845	*vs*
180	0·4838	413		
360	0·4839	812		
222	0·4896	375	0·4911	*vvs*(*b*)
351	0·4902	781		
411	0·4922	758		
142	0·4948	556	0·4944	*m*
421	0·5026	42	0·5023	*vf*(?)
232	0·5069	232	0·5075	*m*
271	0·5126	37	0·5126	*vf*(?)
431	0·5196	268	0·5199	*m*
152	0·5254	167	0·5282	*m*(*b*)
181	0·5276	137		
361	0·5277	100		
242	0·5303	123		
322	0·5481	254	0·5282	*m*
252	0·5590	22	0·5584	*f*
162	0·5605	41		
281	0·5611	27		
332	0·5637	32	—	—
371	0·5688	44	0·5691	*f*
451	0·5705	42		
380	0·5756	39	0·5752	*f*
262	0·5921	34	0·5923	*f*
—	—	—	0·5985	*w*†
422	0·6209	76	—	—
2,10,0	0·6287	30	—	—
272	0·6290	28		
182	0·6413	20	—	—
362	0·6414	56		
372	0·6756	74	0·6757	*f*
2,11,0	0·6842	24	0·6853	*vf*(?)
192	0·6857	67		

hkl	$1/d_{cal.}$ (Å^{-1})	$mF^{2*}/100$	Powder diagram $1/d_{obs.}$ (Å^{-1}) α_1	α_2	*I*
512	0·6961	15	0·6981		*f*
611	0·6967	31			
522	0·7035	36	—		—
462	0·7046	65	0·7054		*f*
153	0·7053	64			
0,12,0	0·7066	49			
292	0·7118	168	0·7129		*w*
303	0·7128	35			
382	0·7131	127			
532	0·7157	134	0·7154		*w*(*b*)
2,11,1	0·7158	91			
631	0·7163	58			
571	0·7198	84	—		—
0,10,2	0·7238	69	—		—
580	0·7251	50			
163	0·7318	108	0·7342		*w*(*b*)
641	0·7330	36			
333	0·7342	123			
4,10,0	0·7356	118			
2,12,0	0·7402	144	0·7398		*vf*(?)
392	0·7533	71	0·7543	0·7542	*m*
552	0·7535	269			
581	0·7550	117			
2,10,2	0·7566	300			
173	0·7620	482	0·7617	0·7616	*m*
590	0·7647	135	—		—
2,12,1	0·7695	184	0·7714		*ms*
353	0·7712	472			
413	0·7724	458			
562	0·7784	459	0·7784	0·7779	*w*
602	0·7841	226	0·7844	0·7843	*vw*
612	0·7863	187			
433	0·7901	162	—		—
622	0·7929	53	0·7930		*vf*(?)
591	0·7931	242			
183	0·7954	83	0·7957	0·7950	*m*(*b*)
363	0·7955	60			
3,10.2	0·7958	223			
2,13,0	0·7966	304			
711	0·8021	85	0·8038	—	*vw*(?)
2,11,2	0·8033	116			
632	0·8037	140			
572	0·8068	98	0·8067	0·8066	*m*(*b*)
740	0·8069	518			
642	0·8168	106	0·8200	—	*w*(*b*)
731	0·8192	189			
0,12,2	0·8224	114			
2,13,1	0·8239	145	0·8249	—	*w*(*b*)
0,14,0	0·8243	61			
4,12,0	0·8329	66	0·8329		*vf*(?)
5,10,1	0·8336	44			
582	0·8384	158	0·8392		*f*
004	0·8418	1211	0·8423	0·8423	*m*
4,10,2	0·8476	49	→		—
690	0·8476	41			
2,12,2	0·8515	505	0·8521	0·8516	*m*
830	0·8995	30	—		—
2,13,2	0·9010	82			

Table 1 (*cont.*)

hkl	$1/d_{cal.}$ (Å^{-1})	$mF^{2*}/100$	Powder diagram $1/d_{obs.}$ (Å^{-1}) α_1	α_2	*I*
742	0·9101	132			
6,10,1	0·9103	52	0·9105		*vf*(?)
2,15,0	0·9103	130			
840	0·9129	192			
1,15,1	0·9146	73	0·9137	0·9130	*mw*(*b*)
682	0·9147	126			
831	0·9238	165			
0,14,2	0·9256	162	0·9249		*w*(*b*)
6,11,0	0·9258	95			
2,11,3	0·9310	55	—		—
633	0·9314	35			
4,12,2	0·9332	247			
573	0·9340	50	0·9336		*w*(*b*)
2,15,1	0·9343	50			
4,14,0	0·9349	49			
174	0·9438	122	0·9445	—	*vf*(?)
762	0·9474	84	—		—
6,11,1	0·9494	219			
354	0·9512	58	0·9507	0·9507	*w*(*b*)
2,14,2	0·9515	115			
424	0·9576	592	0·9575	0·9574	*w*(*b*)
5,13,1	0·9665	43			
2,16,0	0·9676	28	0·9681	—	*vf*(?)
6,12,0	0·9679	65			
184	0·9709	302			
364	0·9709	593	0·9706‡	0·9704	*ms*(*b*)
1,16,1	0·9716	58			
2,12,3	0·9729	111			
802	0·9773	119	0·9773	0·9774	*f*
812	0·9791	39			
2,16,1	0·9902	49			
6,12,1	0·9905	92	0·9916	0·9918	*w*(*b*)
593	0·9916	146			
782	0·9973	249	0·9975	0·9978	*w*(*b*)
—	—	—	1·0015	—	*vf*(?)
4,15,1	1·0094	45			
733	1·0126	114	1·0129	1·0139	*vw*(*b*)
5,14,1	1·0138	28			
2,13,3	1·0165	87	—		—
4,14,2	1·0253	174	1·0272		*vw*(*b*)
1,17,1	1·0288	159			
7,10,2	1·0580	94	—		—
3,16,2	1·0836	98	—		—
—	—	—	1·0874		*f*
1,17,2	1·0915	145	1·0917	1·0928	*vw*
932	1·0922	69			
6,13,2	1·0958	156	—		—
980	1·0984	36			
833	1·0990	100	1·0991	1·1005	*vw*
0,12,4	1·0991	36			
942	1·1033	62	—		—
6,15,0	1·1035	53			
8,11,1	1·1143	125	1·1151	—	*vf*(?)
952	1·1173	107	1·1174‡	—	*vw*
4,10,4	1·1180	86			
6,11,3	1·1206	132			
2,12,4	1·1210	105	1·1208‡	1·1213	*w*
4,16,2	1·1221	125			
5,15,2	1·1230	90			
10,1,1	1·1239	80	—		—
1,19,0	1·1242	115			
—	—	—	1·1268	1·1279	*f*
962	1·1343	90	1·1352	1·1352	*w*
175	1·1355	175			
594	1·1373	99	—		—
6,14,2	1·1377	57			
8,10,2	1·1410	58			
355	1·1417	172	1·1414	1·1417	*w*
415	1·1425	167			
5,17,0	1·1427	111			
972	1·1540	124			
435	1·1546	59	1·1546	—	*vw*
6,12,3	1·1556	56			
2,13,4	1·1590	222	1·1584‡	1·1589	*w*
744	1·1661	378	1·1658	1·1653	*mw*
5,16,2	1·1699	95	1·1692	1·1702	*w*(*b*)
6,16,1	1·1702	119			
—	—	—	1·1735	—	*vf*(?)
982	1·1763	184	1·1769‡	1·1780	*vw*
9,11,0	1·1849	86			
3,19,1	1·1854	179	1·1851	—	*vw*(*b*)
10,2,2	1·1860	82			
3,18,2	1·1874	86	1·1883‡		*w*(*b*)
1,17,3	1·1886	96			
1,20,1	1·2014	133	1·2015		*f*
5,18,1	1·2130	75	—		—
10,8,1	1·2172	38			
5,15,3	1·2176	26	1·2173	—	*vf*(?)
5,17,2	1·2178	24			
11,2,0	1·2185	169	1·2186	1·2191	*vw*
6,16,2	1·2257	147	1·2259	—	*vf*(?)
9,10,2	1·2282	101	1·2286‡	1·2287	*f*
3,17,3	1·2288	24			
—	—	—	1·2356	—	*f*
2,15,4	1·2399	95	1·2401	—	*vw*
3,19,2	1·2402	133			
10,9,1	1·2412	95	—		—
844	1·2418	140	1·2417‡	1·2411	*mw*
5,19,0	1·2472	49	1·2477	—	*vf*(?)
10,10,0	1·2499	39	—		—
6,11,4	1·2513	70	1·2512	—	*vw*
1,20,2	1·2554	126	1·2553‡	—	*w*
9,11,2	1·2575	56			
4,14,4	1·2581	35	1·2581‡	—	*w*
1,21,1	1·2591	30			
006	1·2628	176			
11,6,0	1·2632	44	1·2633	—	*vw*
8,11,3	1·2634	76			
5,18,2	1·2666	89	1·2668‡	—	*w*
10,1,3	1·2719	49	1·2716	—	*f*(*b*)
3,18,3	1·2772	24			
585	1·2779	26	—		—
8,14,2	1·2785	26			
3,21,0	1·2800	29	—		—
6,12,4	1·2828	48	1·2828	—	*w*(*b*)
216	1·2832	68			
046	1·2845	27	—		—
2,12,5	1·2865	40	1·2865‡	—	*w*(*b*)
226	1·2873	50			
11,2,2	1·2891	23	1·2892‡	—	*w*(*vb*)
146	1·2893	74			

* These figures are based on single-crystal observed structure factors. (Calculated structure factors were used for (002), (004), and (006).) Figures for $l = 4$, 3 and 5, and 6 were scaled from figures for corresponding planes with $l = 0$, 1, and 2 respectively. m = multiplicity.

† These lines are presumably due to an impurity; they correspond in spacing to strong lines of Cr_2O_3.

‡ Each of these lines presumably contains an α_2 contribution from the preceding line, but is here calculated as if α_2 were absent or inconsequential.

Refinements of lattice constants

Powder photographs, obtained with a finely pulverized specimen of the alloy in a 0·15 mm. pyrex capillary tube mounted in a 114·59 mm. Philips powder camera, with nickel-filtered copper radiation, were used as the basis of the refinement of the lattice constants. Because of the low symmetry and large size of the unit cell it was evident that resolution, except at low angles, would not be possible without information from another source regarding the expected intensities of reflection. For this purpose, single-crystal intensity data obtained by Weissenberg photography for reciprocal lattice layers $l = 0$, 1, and 2 were used. For higher layers, use was made of the fact that in this structure, as in that of the σ phase, the atoms are confined to layers parallel to (001) planes, rather precisely quartering the cell; thus, except for normal decline, the corrected intensities for layer $l\pm4$ are equal to corresponding ones for layer l. Factors of proportionality among the layers were estimated by a least-squares method from incomplete intensity data for layers 3 and 5 in relation to the complete data for layer 1, assuming the form factors to be proportional to a Gaussian function of l. When the estimated corrected intensities were multiplied by the appropriate powder multiplicities and tabulated with reciprocal spacings ($1/d$) calculated from the preliminary single-crystal lattice constants, it became possible to identify most of the observed powder lines. This made possible successive adjustments in lattice constants, leading ultimately to the identification of nearly all powder lines out to a spacing of 1·29 Å^{-1} ($\sin\theta = 0{\cdot}994$), which constituted a practical limit to both the powder data and the single-crystal data. The final assignment of values for the cell constants, made to provide the best possible fit with observed lines at high angles (especially (11,2,0), (1,20,2), and (146)), is as follows:

$$a_0 = 9{\cdot}070 \pm 0{\cdot}003, b_0 = 16{\cdot}983 \pm 0{\cdot}006, c_0 = 4{\cdot}752 \pm 0{\cdot}002 \text{ Å}.$$
$$(\lambda_{\text{Cu } K\alpha_1} = 1{\cdot}54050 \text{ Å};\ \lambda_{\text{Cu } K\alpha_2} = 1{\cdot}54434 \text{ Å}.)$$

In Table 1 the indexed powder diagram is presented. The calculated reciprocal spacings in this table are based on the final lattice constants just given. Planes with intensities much lower than the faintest observed powder lines are omitted; the limiting numerical value varies with angle, but is always taken low enough so that no observed lines in the neighborhood are below it and some unobserved ones are above it. It will be seen that the observed powder diagram is in excellent detailed agreement with the diagram predicted with the single-crystal intensities; it is also in agreement with the diagram given by Rideout *et al.* (1951). The agreement demonstrates also that the microscopic single-crystal fragments selected from the pulverized material and used for the structure determination are reasonably typical of the bulk material, and not accidentally selected particles of some minor constituent.

Of the seven lines which could not be identified as *P*-phase lines, the two first and strongest corresponded closely with the strongest lines of chromic oxide, Cr_2O_3. The others, which were very much fainter, were not identified.

The density was determined by displacement of water in a pycnometer. Five determinations gave a mean value of 9·064 g.cm.$^{-3}$, with an average deviation of 0·013. With the composition stated above, this corresponds to 54·7 atoms per unit cell. The space group requires that the number of atoms be a multiple of four, and the nearest multiple is 56, which is the number of atoms shown to be present by the structure determination. This poor agreement suggested that the stated composition is in error, but chemical analysis of the alloy for molybdenum confirmed (within 1%) the stated value of 55 weight%. However, a small residue, insoluble in acid, was identified by powder photography as Cr_2O_3. Other experiments showed that the amount of slag or oxide present is at least 2% and probably more; if the order of 4% of the material is assumed to be surface oxide or slag inclusions, the discrepancy between the observed density and the X-ray density (9·28 g.cm.$^{-3}$) may be explained.

Refinement of parameters

The choice of refinement method was determined in part by the circumstances of the structure determination. It was evident from inspection of the intensities of reflection on the ($hk0$) reciprocal-lattice net that the structure is closely similar to the σ-phase structure, as may be seen from Fig. 1. The determination

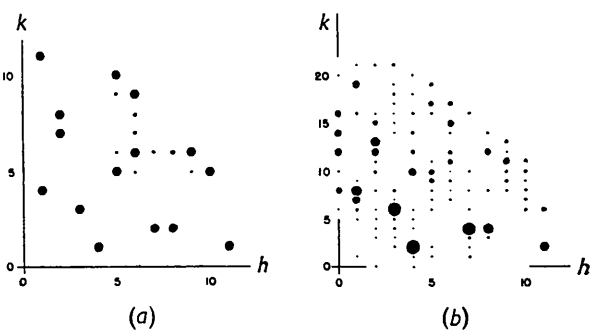

Fig. 1. The ($hk0$) reciprocal-lattice layers of (*a*) the σ phase (e.g., Fe–Cr) and (*b*) the *P* phase (Mo–Ni–Cr). The intensities are shown qualitatively by the sizes of the dots. (Note: The layer for the *P* phase is drawn as if the b/a ratio were exactly 2; as this ratio is in fact 1·87, the figure should be expanded 7% in the vertical direction.)

of the structure consisted basically of the trial-and-error juxtapositioning of two differently oriented fragments of the σ phase (about one unit cell in size), in accordance with the b glide. A number of possible ways of doing this became evident, and these differed

mainly according to the selection of atoms to be designated as belonging to the subsidiary layers (atoms XI and XII). Therefore, at least throughout the period during which the structure-factor agreement was rough, refinement was carried out with the use of (*hk*2) intensity data, which are sensitive to the selection of the subsidiary atoms while (*hk*0) data are not especially so. A generalized projection calculated with (*hk*2) data alone gives peaks corresponding to the atoms on both the main layers and the subsidiary layers, but with opposite sign. As the atoms are all reasonably well resolved in projection (except the subsidiary atoms, of which pairs coincide exactly in projection), this circumstance presented no handicap.

Weissenberg photographs were taken of the layers $l = 0$, 1, and 2 with nickel-filtered copper radiation, with a crystal fragment of irregular shape considerably less than 0·1 mm. in size. The intensities were estimated visually on multiple films with an intensity strip, and observed structure factors were calculated. Three successive projections were calculated with (*hk*2) data. In the calculation of the subsequent set of structure factors the atoms were put in with weights, or 'scattering parameters', proportional to the heights of the peaks on the third projection. The *R* factors then obtained for (*hk*0) and (*hk*2) structure factors were 20 and 19% respectively, unobserved planes having been omitted from the calculations.

The signs from the above set of structure factors were then used in a pair of generalized projections, designated 'Fourier IV', calculated with both (*hk*0) and (*hk*2) data. One of these, $\Sigma(F_{hk0}-F_{hk2})$, gave positive peaks due to atoms on the two main layers ($z = \frac{1}{4}$ and $\frac{3}{4}$), while the other, $\Sigma(F_{hk0}+F_{hk2})$, gave positive peaks due to atoms on the two subsidiary layers ($z = 0{\cdot}00$ and 0·50). The computations were carried out on the MIT Whirlwind computer, with a program worked out by Prof. S. M. Simpson, Jr., of the Department of Geology of this Institute. (The original project of including (*hk*1) data, not so much in order to improve resolution on the main layers as to use more data in refinement, was abandoned because the computer program could not conveniently deal with sine functions.)

Positional parameters were obtained from these projections by a least-squares method analogous to that used in three dimensions by Shoemaker, Donohue, Schomaker & Corey (1950). The Gaussian parameters for each atom were obtained from nine points in a three-by-three grid taken as near as possible to the atomic center. The scattering parameter for each atom was taken to be proportional to the integral of the appropriate Gaussian electron-density function over all two-dimensional space. These scattering parameters were intended to be factors by which the previously used weighted mean atomic form factors (including a temperature factor $\exp(-B\sin^2\theta/\lambda^2)$ with $B = 1{\cdot}1$ Å^2) should be multiplied to obtain the approximately correct values for the respective atoms. They are of course affected in the present case by the fact that in a generalized projection contributions due to scattering matter at different levels are projected with varying weights, the weight in the present case decreasing with a cosine function of the distance away from the plane of the atomic center. Therefore the scattering parameters are normalized to a weighted mean of unity.

The two projections are shown in Fig. 2, and the

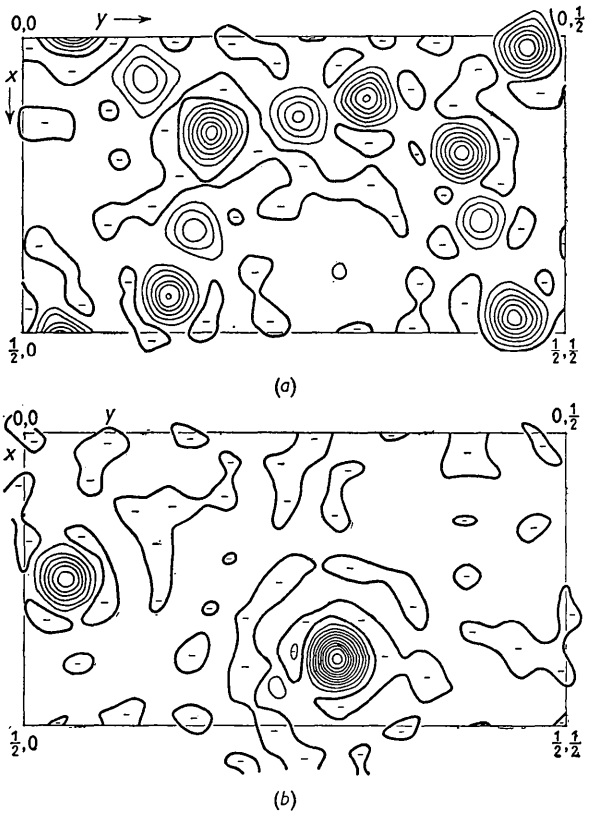

Fig. 2. (*a*) The $\Sigma(F_{hk0}-F_{hk2})$ generalized projection, showing peaks due to atoms lying on the main layers at $z = \frac{1}{4}$ and $z = \frac{3}{4}$. (*b*) The $\Sigma(F_{hk0}+F_{hk2})$ generalized projection, showing peaks due to atoms lying on the subsidiary layers; each peak is due to two atoms, one at $z = 0{\cdot}00$ and one at $z = 0{\cdot}50$.

In both projections the zero-density contours are drawn heavy.

parameters derived from them are listed under 'Fourier IV' in Table 2. It will be observed that small contributions from atoms on the subsidiary layers appear on the main layers, and vice versa; these presumably result from the property of generalized projections mentioned in the previous paragraph. Also worthy of mention are the diffraction effects, which are particularly noticeable around the high peaks on the subsidiary layers.

To correct for shifts in peak centers due to diffraction (finite summation) and peak-overlap effects, as well as to the property of generalized projections mentioned above, the method of Booth (1946) was em-

Table 2. *Atomic parameters in P phase*, Mo–Ni–Cr

			x, *y* parameters*				Scattering parameters†					
Atom	Position	*z*	Initial	Fourier IV	Δ	Final	Fourier IV	Δ	Final	% Mo	C.N.	σ type
I	4(*c*)	¼	0·063 0·118	0·0730 0·1127	−0·0007 −0·0007	0·0737 0·1134	0·93	−0·02	0·95	35	12	*A*
II	4(*c*)	¼	0·150 0·248	0·1369 0·2548	+0·0006 +0·0001	0·1363 0·2547	0·85	−0·02	0·87	20	12	*D*
III	4(*c*)	¼	0·340 0·158	0·3267 0·1566	+0·0010 −0·0012	0·3257 0·1578	0·75	−0·01	0·76	0	12	*D*
IV	4(*c*)	¼	0·590 0·190	0·6063 0·1829	+0·0005 +0·0010	0·6058 0·1819	1·12	−0·06	1·18	78	14	*C*
V	4(*c*)	¼	0·673 0·337	0·6642 0·3262	−0·0008 +0·0009	0·6650 0·3253	1·25	+0·14	1·11	65	15	*B*
VI	4(*c*)	¼	0·443 0·447	0·4751 0·4532	+0·0005 −0·0004	0·4746 0·4536	1·35 (1·27)	−0·06	1·41 (1·30)	100	16	—
VII	4(*c*)	¼	0·190 0·412	0·1984 0·4047	−0·0004 0·0000	0·1988 0·4047	1·22	−0·10	1·32 (1·30)	100	14	*C*
VIII	4(*c*)	¼	0·807 0·082	0·8128 0·0773	−0·0024 −0·0007	0·8152 0·0780	0·68 (0·72)	+0·07	0·61 (0·76)	0	12	*D*
IX	4(*c*)	¼	0·943 0·368	0·9382 0·3655	−0·0001 +0·0005	0·9383 0·3650	1·13	−0·05	1·18	78	14	*C*
X	4(*c*)	¼	0·513 0·027	0·5201 0·0346	−0·0001 −0·0009	0·5202 0·0355	1·34 (1·27)	−0·03	1·37 (1·30)	100	15	—
XI	8(*d*)	0·9986‡	0·250 0·535	0·2512 0·5377	+0·0008 +0·0002	0·2504 0·5375	0·66 (0·72)	+0·07	0·59 (0·76)	0	12	—
XII	8(*d*)	0·0008‡	0·380 0·288	0·3865 0·2883	−0·0003 0·0000	0·3868 0·2883	1·03	−0·01	1·04	52	14	*E*

* For each atom the *y* parameter lies directly beneath the corresponding *x* parameter. Δ values are apparent errors due to non-convergence and peak-overlap effects, as determined by the Booth method.

† Parenthesized values in the 'Fourier IV' column are assumed limiting values, used instead of the unparenthesized values lying directly above them in the calculation of the penultimate set of structure factors, which were used in the 'calculated Fourier' to obtain the Δ values. Parenthesized values in the 'Final' column are also assumed limiting values (differing from the others in that dispersion corrections are taken into account) used instead of the unparenthesized ones in calculating the final set of structure factors (Table 3) and the % Mo in the next column.

‡ The two *z* parameters are not significantly different from 0·00 (see text).

ployed. A pair of generalized projections, 'Fourier V', paralleling Fourier IV but with calculated structure amplitudes as well as signs, was prepared, with the omission of the same planes that were omitted in the calculation of Fourier IV. The parameters going into the calculation of these structure factors were those given by Fourier IV, except that some of the scattering-factor parameters which appeared to be unreasonably high or low were replaced by limiting values (the parenthesized figures in Table 2). The resulting projections resembled those of Fourier IV very closely, even in the locations and heights of minor maxima and minima in the background. Parameters were obtained as before, and from these were subtracted the parameters going into the structure-factor calculations, in order to yield parameter shifts represented by 'Δ' in Table 2. These shifts were subtracted from the parameters from Fourier IV, to give the values listed under 'Final' in Table 2.

As in the case of the uncorrected parameters, some of the scattering parameters appeared unreasonably high or low. In the calculation of the final set of structure factors, given in Table 3, these were replaced by limiting values (parenthesized in Table 2), calculated this time with due account of anomalous *K*-electron scattering, which had been neglected up to this point. The lower limit was taken as the ratio of the corrected scattering factor for chromium to the corrected weighted mean, the upper limit similarly for molybdenum, considering in all cases only the scattering factor for zero scattering angle since the scattering parameter was determined as the total effective quantity of scattering matter in the atomic Fourier peak. However, the introduction of these limits destroyed the normalization. Moreover, in the final structure-factor calculation, the previously used weighted mean form factor, uncorrected for anomalous scattering, was multiplied by the scattering parameters. As a result, the structure factors are on the average scaled about 8% high (2% from the first cause, 6% from the second), and the corrected intensities of Table 1 are accordingly about 16% too high, without taking

Table 3. *Observed and calculated structure factors*

k	F_o	F_c
	0k0	
0		475
2	—	2
4	—	− 2
6	10	2
8	52	−49
10	24	−25
12	50	−50
14	56	−62
16	41	−38
18	—	−11
20	14	2
	1k0	
1	6	− 4
2	—	6
3	—	2
4	—	1
5	18	10
6	26	26
7	65	−69
8	102	−117
9	24	25
10	—	−17
11	—	− 6
12	—	3
13	—	− 6
14	—	12
15	—	12
16	31	30
17	—	11
18	—	− 5
19	54	49
20	—	2
21	23	−25
	2k0	
0	10	9
1	—	− 8
2	—	8
3	10	−11
4	14	12
5	20	13
6	13	17
7	—	8
8	15	17
9	—	6
10	27	−23
11	24	15
12	60	−65
13	88	−98
14	—	4
15	57	73
16	27	23
17	—	−12
18	—	6
19	—	− 3
20	—	1
21	19	9
	3k0	
1	—	− 4
2	10	1
3	21	8
4	31	−28
5	44	−45
6	143	155
7	13	11
8	32	37
9	—	− 4
10	—	14
11	—	9
12	—	5
13	—	4
14	22	−10
15	20	−20
16	22	−18
17	21	15
18	30	−29
19	21	22
20	—	− 8
21	27	37
	4k0	
0	21	−22
1	34	30
2	143	159
3	—	− 5
4	13	12
5	13	0
6	18	− 9
7	—	−10
8	—	− 3
9	—	3
10	54	−57
11	—	4
12	41	−44
13	—	−12
14	35	−37
15	—	0
16	26	−31
17	—	− 4
18	16	−16
19	—	−17
20	14	11
	5k0	
1	13	−17
2	22	−25
3	—	5
4	—	− 8
5	—	5
6	17	14
7	24	19
8	35	38
9	58	−66
10	41	−47
11	17	15
12	—	5
13	—	4
14	—	13
15	—	18
16	31	−22
17	53	44
18	—	− 3
19	35	−41
	6k0	
0	—	1
1	—	1
2	—	10
3	—	2
4	—	3
5	—	−15
6	—	− 3
7	17	16
8	24	−24
9	32	31
10	22	−24
11	49	−56
12	40	52
13	—	5
14	21	− 9
15	36	−38
16	—	−10
17	29	36
18	—	3
	7k0	
1	24	11
2	19	− 8
3	26	−27
4	114	131
5	—	1
6	17	16
7	—	− 3
8	23	26
9	—	− 5
10	21	22
11	—	7
12	—	8
13	—	7
14	—	− 1
15	—	12
16	14	−18
	8k0	
0	—	11
1	—	− 4
2	—	− 9
3	27	38
4	69	87
5	—	−12
6	—	7
7	—	− 6
8	27	−27
9	—	− 9
10	—	−16
11	—	− 7
12	43	−40
13	—	3
14	14	−19
	9k0	
1	—	− 8
2	—	2
3	—	− 9
4	—	− 6
5	—	8
6	—	3
7	—	− 2
8	30	19
9	31	26
10	30	27
11	46	−43
12	16	−16
13	11	17
	10,k,0	
0	—	9
1	—	5
2	—	−13
3	—	− 6
4	—	− 6
5	—	3
6	15	−14
7	14	2
8	21	−20
9	22	−23
10	32	42
11	15	24
	11,k,0	
1	—	− 1
2	65	73
3	—	− 1
4	—	4
5	—	− 8
6	34	39
	0k1	
2	14	9
4	—	10
6	18	−20
8	13	−13
10	—	8
12	21	−25
14	—	− 4
16	—	− 7
18	—	− 8
20	16	−19
	1k1	
0	6	− 6
1	7	− 1
2	12	− 9
3	—	1
4	—	1
5	36	42
6	47	56
7	100	140
8	41	−52
9	—	− 2
10	—	0
11	—	− 3
12	—	− 3
13	17	13
14	—	10
15	30	−24
16	27	26
17	44	−36
18	—	− 7
19	—	− 7
20	40	−40
21	19	−21
	2k1	
1	—	−10
2	14	−10
3	10	− 2
4	—	1
5	—	− 8
6	—	− 4
7	21	−23
8	18	22
9	13	−10
10	—	− 2
11	34	32
12	48	−60
13	42	52
14	24	−22
15	25	−24
16	25	22
17	—	−10
18	—	3
19	—	8
20	—	3
	3k1	
0	38	31
1	17	− 6
2	9	−12
3	50	57
4	31	−28
5	99	128
6	35	44
7	23	−26
8	12	−15
9	14	15
10	—	8
11	20	13
12	—	4
13	—	2
14	—	4
15	—	− 2
16	—	− 6
17	22	−11
18	22	−22
19	47	−43
20	12	−10
	4k1	
1	98	−122
2	23	26
3	58	60
4	—	− 2
5	23	29
6	—	− 6
7	—	− 5
8	—	− 9
9	24	16
10	20	−21
11	—	− 7
12	—	5
13	—	13
14	—	−16
15	24	24
16	—	− 5
17	—	− 1
18	—	− 3
19	12	8
	5k1	
0	—	2
1	—	7
2	11	−15
3	—	3
4	11	10
5	18	12
6	—	− 1
7	32	28
8	38	45
9	55	74
10	24	−29
11	—	4
12	15	− 2
13	23	−22
14	19	17
15	24	−21
16	—	− 7
17	21	−20
18	31	−31
19	—	− 2
	6k1	
1	20	−15
2	15	14
3	27	−27
4	21	−19
5	—	−12
6	14	8
7	19	−19
8	—	−18
9	—	7
10	26	−20
11	52	64
12	34	34
13	28	22
14	—	−10
15	—	− 3
16	38	−37
17	—	− 5
18	13	14
	7k1	
0	—	− 6
1	32	33
2	—	4
3	49	64
4	—	8
5	—	−16
6	14	− 6
7	—	8
8	14	16
9	—	3
10	—	− 5
11	18	23
12	—	− 2
13	—	− 2
14	—	8
15	—	− 3
16	—	4
17	12	−17
	8k1	
1	19	−17
2	17	−15
3	45	−54
4	16	11
5	19	16
6	—	2
7	15	14
8	14	−10
9	—	− 3
10	—	− 2
11	40	33
12	16	−17
13	22	14
14	—	4
15	—	5
	9k1	
0	—	2
1	—	8
2	17	13
3	20	16
4	18	−21
5	—	4
6	—	5
7	15	− 3
8	—	10
9	—	8
10	21	27
11	19	17
12	—	− 5
13	17	−1

Table 3 (*cont.*)

k	F_o	F_c
	10,*k*,1	
1	32	−29
2	14	−15
3	14	−10
4	29	21
5	22	−24
6	13	−12
7	12	13
8	22	−22
9	35	43
	11,*k*,1	
0	14	− 8
1	17	17
2	—	− 2
3	14	−20
4	13	11
5	13	−11
6	7	8
	0*k*2	
0	Str.	−176
2	16	−24
4	72	93
6	11	− 2
8	—	− 3
10	42	36
12	53	−58
14	64	69
16	30	−30
18	11	12
20	10	2
	1*k*2	
1	16	21
2	—	− 7
3	40	−48
4	84	−102
5	46	53
6	23	−27
7	11	− 3
8	16	− 2
9	29	24
10	—	9
11	20	−18
12	26	−26
13	—	5
14	12	−12
15	—	6
16	18	14
17	43	−37
18	12	6
19	14	−15
20	40	49
	2*k*2	
0	59	−61
1	80	94
2	69	−77
3	54	−58
4	39	−40
5	17	19
6	21	−25
7	19	2
8	—	− 2
9	46	−44
10	62	61
11	38	41
12	80	90
13	32	32
14	38	41
15	18	−22
16	—	1
17	24	−14
18	11	10
19	12	8
	3*k*2	
1	—	− 8
2	56	60
3	20	22
4	10	15
5	8	− 2
6	26	−10
7	30	30
8	40	−38
9	30	−25
10	53	57
11	11	7
12	—	− 3
13	—	− 3
14	—	− 6
15	—	7
16	35	22
17	12	5
18	33	−30
19	41	−40
	4*k*2	
0	11	0
1	—	− 2
2	31	−15
3	18	−12
4	21	−18
5	13	8
6	29	24
7	10	11
8	10	10
9	14	−12
10	25	−22
11	—	11
12	56	52
13	—	− 4
14	47	−46
15	14	12
16	40	35
17	—	− 4
18	—	−12
19	11	17
	5*k*2	
1	14	− 1
2	21	−15
3	41	38
4	—	−11
5	58	−61
6	76	−84
7	35	40
8	45	−50
9	15	14
10	11	− 2
11	—	9
12	12	−11
13	—	− 4
14	—	− 3
15	34	−35
16	34	27
17	17	−12
18	34	40
	6*k*2	
0	76	−75
1	48	−57
2	26	−26
3	42	40
4	36	−44
5	—	− 7
6	—	0
7	19	−21
8	40	42
9	—	− 2
10	25	32
11	—	11
12	—	4
13	44	35
14	27	21
15	—	3
16	43	43
17	14	−14
	7*k*2	
1	—	− 7
2	—	0
3	17	13
4	41	−39
5	14	12
6	32	−26
7	12	−11
8	56	56
9	14	15
10	34	−25
11	12	−10
12	12	12
13	—	− 6
14	—	5
15	—	− 6
16	11	−21
	8*k*2	
0	54	70
1	22	−24
2	—	4
3	—	−12
4	29	−34
5	—	2
6	—	− 6
7	—	4
8	—	1
9	23	22
10	27	19
11	12	−13
12	19	−21
13	18	18
14	18	20
	9*k*2	
1	13	19
2	—	−14
3	29	−20
4	28	−24
5	36	33
6	34	−28
7	40	−39
8	48	−49
9	—	8
10	36	−42
11	26	22
12	4	6
	10,*k*,2	
0	—	− 9
1	24	24
2	32	−38
3	11	−17
4	—	3
5	—	7
6	—	5
7	—	1
8	13	19
	11,*k*,2	
1	—	0
2	17	−40

account of the angular dependence of the anomalous scattering correction (absorbed, in effect, into the temperature factor).

In Table 3 the observed and final calculated structure factors, scaled on the basis of one asymmetric unit, are compared. The agreement is generally satisfactory, though there are a few rather large discrepancies, some of which may be due to absorption (despite the small size of the crystal, absorption effects may arise from its irregular shape, as the calculated linear absorption coefficient is 1300 cm.$^{-1}$). The strong reflections show some evidence of secondary extinction. The final R factors for ($hk0$), ($hk1$), and ($hk2$) data, omitting all unobserved planes, were respectively 16·6, 19·8, and 16·5%, with a weighted average of 17·5%, representing a very slight improvement over the average factor (17·8%) for the previous set of structure factors (following Fourier IV).

In order to permit a refinement of the two z parameters by least squares, the intensities of a number of reflections ($hk3$) and ($hk5$) were estimated from Weissenberg photographs of the same crystal reoriented to permit rotation around the a axis. Forty observational equations were reduced to two normal equations in the usual way, and these were solved to obtain the two z parameters. The two values, −0·0014 for XI and +0·0008 for XII, are very close to the 'ideal value' of exactly zero. Since, however, the apparent standard errors to which they are subject are 0·0064 and 0·0043 respectively, the parameters are not regarded as significantly different from zero. The large standard errors are due in large part to the smallness of the number of suitable data available for the calculation. The uncertainty in the z parameters is perhaps much smaller than that indicated by the standard error calculated from residuals, in view of the probable tendency of these atoms to form bonds of equal length with the atoms directly above and below them; if a z parameter were to differ from zero by as much as 0·0064 (or 0·030 Å) the distances above and below the atom would differ by 0·12 Å, or over 4%. Accordingly, these parameters were given the value zero in the calculation of the structure factors given in Table 3 and in the calculation of the interatomic distances given in Table 4.

The probable errors in the x, y, and scattering parameters may conservatively be taken as comparable with the averages of the Booth shifts. Limits of error,

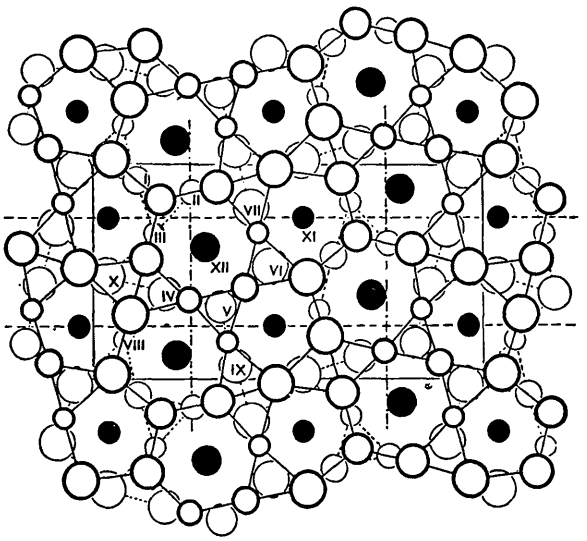

Fig. 3. The crystal structure of the P phase, Mo–Ni–Cr, viewed along the **c** axis. The unit cell is outlined in thin solid line; the origin is at upper left, with x running downwards, y toward the right. Light circles joined by dashed lines are atoms on one main layer at $z = \frac{1}{4}$; heavy circles joined by solid lines are atoms on the other main layer at $z = \frac{3}{4}$. Each solid black circle represents two atoms in superposition, one on one subsidiary layer at $z = 0{\cdot}00$ and one on the other subsidiary layer at $z = 0{\cdot}50$. The diameter of each circle is proportional to the final 'scattering parameter' (except where replaced by a parenthesized limiting value) given for the corresponding atom in Table 2.

taken as three times the probable error, may be taken as 0·02 Å for the positional parameters, or 0·03 Å for the interatomic distances, and about 0·2 for the scattering parameters, or about 30% in the figures given for the percentage content of molybdenum in the atomic sites.

Discussion

The P-phase structure bears close resemblances to the σ-phase structure, a fact that was very useful in the structure determination above described. Grossly, the P-phase structure differs from the σ-phase structure in that the two orientations of pseudohexagonal ('subcell') axes that are found on alternating main layers in the σ phase are present in adjacent regions on every main layer of the P phase. At the joins between the differently oriented fields on a given main layer, where the pseudohexagonal axes appear to 'step' from layer to layer, pentagonal holes replace some of the σ-phase hexagonal holes, resulting in some apparent distortion of the pseudohexagonality and also resulting in an increase in the proportion of 12-coordinated atoms in the structure from one-third to three-sevenths. However, the distortion does not result in poorer packing, as will be seen in the discussion that follows. The types of atomic coordination found in the P phase are the same as those found in the σ phase (and, as shown by the last column of Table 2, in most cases are even similarly located with respect to one another), except that in the P phase there is a kind of coordination, 16-fold, not found in the σ phase. Other differences between the two structures are relatively minor.

We have pointed out (Shoemaker, Brink & Fox, 1955) that the α-manganese or χ-phase structure has layers resembling very closely those existing in the σ phase, and indeed the two main layers in one half of the α-manganese cubic cell (between, say, $z = 0$ and $z = \frac{1}{2}$) resemble the two main layers of a rather distorted σ-phase unit cell, as shown in Fig. 4. The P-phase structure has in common with the α-manganese structure, besides the resemblances in the layers, the occurrence of 16-fold coordination (the atoms represented by large circles in Fig. 4).

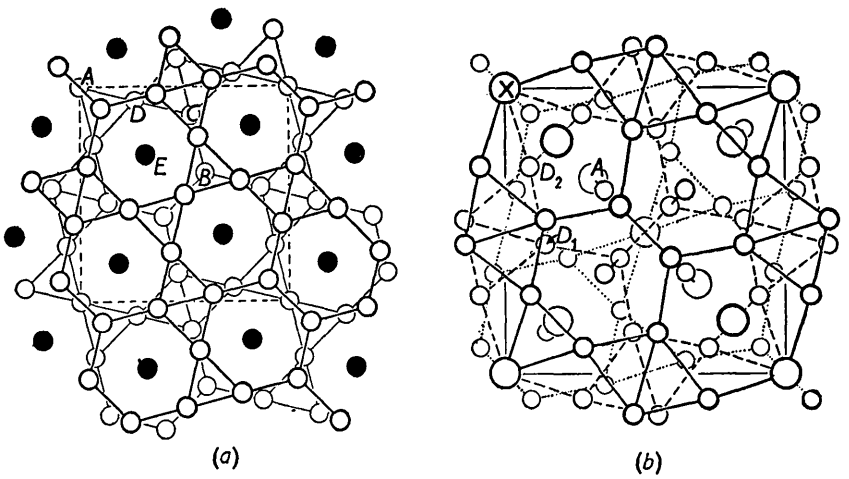

Fig. 4. (*a*) The crystal structure of the σ phase (e.g., Fe–Cr), and (*b*) that of α-manganese and of the χ phase (e.g., $Fe_{36}Cr_{12}Mo_{10}$), for comparison with the P-phase structure shown in Fig. 3. Compare one unit cell of the σ phase, or the lower (more lightly drawn) layers of those shown for α-manganese (representing one half of the body-centered cubic unit cell), with the leftmost half of the unit cell of the P phase.

It is of interest to examine the coordination types in terms of the coordination polyhedra, the vertices of which are usually taken to be the near neighbors (ligates) of the atoms concerned, but will here be taken to be the termini of the ligand radii directed toward these neighbors. This latter definition is the one more appropriate to a discussion of bond lengths as the sum of metallic radii, where a given atom with

Table 4. *Observed and calculated interatomic distances*

All distances are in Ångström units (Å). Ligands are grouped according to layers on which the ligate atoms are found. Symbol(s) following each ligate give the relation to the numbered equivalent atom in Fig. 3 (1 = identity; t = lattice translation; i = inversion; m = mirror reflection; b = b-glide reflection; n = n-glide reflection). Asterisks indicate six-coordinated ligands. All averages of distances and deviations are weighted according to the numbers of times the respective distances occur.

		$D_{obs.}$	$D_{cal.}$	Δ
Atom I				
II	1	2·466	2·384	0·082
III	1	2·407	2·384	0·023
VI(b)	1	2·749	2·805	0·056
VIII(t)	1	2·420	2·384	0·036
XI(b, bm)	2	2·370	2·384	0·014
XII(n, nm)	2	2·659	2·637	0·022
V(n)	2	2·723	2·743	0·020
VI(n)	2	2·784	2·805	0·021
	12	2·593	—	0·029
Atom II				
I	1	2·466	2·384	0·082
III	1	2·379	2·384	0·005
VII	1	2·610	2·637	0·027
IX(t)	1	2·595	2·637	0·042
XII(1, m)	2	2·627	2·637	0·010
XII(n, nm)	2	2·658	2·637	0·021
IV(n)	2	2·623	2·637	0·014
V(n)	2	2·749	2·743	0·006
	12	2·614	—	0·022
Atom III				
I	1	2·407	2·384	0·023
II	1	2·379	2·384	0·005
IV	1	2·573	2·637	0·064
X	1	2·725	2·743	0·018
XI(b, bm)	2	2·462	2·384	0·078
XII(1, m)	2	2·575	2·637	0·062
V(n)	2	2·802	2·743	0·059
IX(n)	2	2·615	2·637	0·022
	12	2·583	—	0·046
Atom IV				
III	1	2·573	2·637	0·064
*V	1	2·494	2·536	0·042
VIII	1	2·592	2·637	0·045
*X	1	2·605	2·536	0·069
XII(1, m)	2	2·936	2·890	0·046
XII(n, nm)	2	2·857	2·890	0·033
II(n)	2	2·623	2·637	0·014
VII(n)	2	2·919	2·890	0·029
IX(n)	2	2·930	2·890	0·040
	14	2·771	—	0·039
Atom V				
*IV	1	2 494	2·536	0·042
*VI	1	2·780	2·772	0·008
*IX	1	2·569	2·536	0·033
XI(i, im)	2	2·726	2·728	0·002
XII(1, m)	2	2·859	2·981	0·122
XII(n, nm)	2	3·030	2·981	0·049
I(n)	2	2·723	2·743	0·020
II(n)	2	2·749	2·743	0·006
III(n)	2	2·802	2·743	0·059
	15	2·775	—	0·040
Atom VI				
I(b)	1	2·749	2·805	0·056
*V	1	2·780	2·772	0·008
*VII	1	2·636	2·660	0·024
VIII(b)	1	2·846	2·805	0·041
XI(1, m)	2	2·753	2·805	0·052
XI(i, im)	2	2·767	2·805	0·038
XII(1, m)	2	3·151	3·058	0·093
I(n)	2	2·784	2·805	0·021
*VI(i)	2	2·888	2·856	0·032
VIII(n)	2	2·833	2·805	0·028
	16	2·835	—	0·041
Atom VII				
II	1	2·610	2·637	0·027
*VI	1	2·636	2·660	0·024
*IX(t)	1	2·457	2·424	0·033
X(b)	1	2·980	2·981	0·001
XI(1, m)	2	2·592	2·637	0·045
XII(1, m)	2	2·868	2·890	0·022
IV(n)	2	2·919	2·890	0·029
VIII(n)	2	2·617	2·637	0·020
X(n)	2	3·050	2·981	0·069
	14	2·770	—	0·032
Atom VIII				
I(t)	1	2·420	2·384	0·036
IV	1	2·592	2·637	0·045
VI(b)	1	2·846	2·805	0·041
X	1	2·771	2·743	0·028
XI(n, nm)	2	2·367	2·384	0·017
XII(n, nm)	2	2·644	2·637	0·007
VI(n)	2	2·833	2·805	0·028
VII(n)	2	2·617	2·637	0·020
	12	2·629	—	0·024

Table 4 (*cont.*)

Atom IX

		$D_{obs.}$	$D_{cal.}$	Δ
II(t)	1	2·595	2·637	0·042
*V	1	2·569	2·536	0·033
*VII(t)	1	2·457	2·424	0·033
X(b)	1	2·920	2·981	0·061
XI(i, im)	2	2·661	2·637	0·024
XII(n, nm)	2	2·900	2·890	0·010
III(n)	2	2·615	2·637	0·022
IV(n)	2	2·930	2·890	0·040
X(n)	2	3·009	2·981	0·028
	14	2·769	—	0·030

Atom X

III	1	2·725	2·743	0·018
*IV	1	2·605	2·536	0·069
VII(b)	1	2·980	2·981	0·001
VIII	1	2·771	2·743	0·028
IX(b)	1	2·920	2·981	0·061
XI(b, bm)	2	2·727	2·743	0·016
XI(n, nm)	2	2·703	2·743	0·040
VII(n)	2	3·050	2·981	0·069
IX(n)	2	3·009	2·981	0·028
*X(i)	2	2·690	2·648	0·042
	15	2·824	—	0·038

Atom XI

		$D_{obs.}$	$D_{cal.}$	Δ
I(b)	1	2·370	2·384	0·014
III(b)	1	2·462	2·384	0·078
VI	1	2·753	2·805	0·052
VII	1	2·592	2·637	0·045
X(b)	1	2·727	2·743	0·016
V(i)	1	2·726	2·728	0·002
VI(i)	1	2·767	2·805	0·038
VIII(n)	1	2·367	2·384	0·017
IX(i)	1	2·661	2·637	0·024
X(n)	1	2·703	2·743	0·040
XI(m, m')	2	2·376	2·384	0·008
	12	2·573	—	0·028

Atom XII

II	1	2·627	2·637	0·010
III	1	2·575	2·637	0·062
IV	1	2·936	2·890	0·046
V	1	2·859	2·981	0·122
VI	1	3·151	3·058	0·093
VII	1	2·868	2·890	0·022
I(n)	1	2·659	2·637	0·022
II(n)	1	2·658	2·637	0·021
IV(n)	1	2·857	2·890	0·033
V(n)	1	3·030	2·981	0·049
VIII(n)	1	2·644	2·637	0·007
IX(n)	1	2·900	2·890	0·010
*XII(m, m')	2	2·376	2·424	0·048
	14	2·751	—	0·042

Number of different distances	58
Average distance	2·710
Largest distance	3·151
Smallest distance	2·367
Average deviation between $D_{obs.}$ and $D_{cal.}$	0·036
Largest deviation	0·122

a given coordination type may have, depending on the symmetry of its coordination, one or more characteristic radii. The structure may then be regarded as a close packing of the respective conjugate polyhedra (see Wells (1956), p. 32, pp. 56 ff.), or even of spheres and correspondingly distorted spheres.

The coordination polyhedra present in the σ and P phases have roughly equilateral triangular faces, and fivefold and/or sixfold vertices. (A fivefold vertex is a vertex where five edges come together, and so on.) We shall speak of the radius to a fivefold vertex as a *five-coordinated radius* (r or r'), and of the radius to a sixfold vertex as a *six-coordinated radius* (r^*). Clearly, in the absence of considerable distortion, a five-coordinated radius should form a ligand only with another five-coordinated radius and a six-coordinated radius only with another six-coordinated radius; hence we may speak of *five-coordinated ligands* and *six-coordinated ligands*. These names are not wholly satisfactory but are descriptive (since a five-coordinated ligand has a ring of five atoms around its center), and are convenient for the present discussion. The polyhedra present in the P and σ phases are the following, variously distorted in slight degree:

Coordination 12 (I, II, III, VIII, XI in P phase; A and D in σ phase; D_2 in α-Mn): Regular icosahedron, point symmetry I_h; twelve fivefold vertices, represented by a single five-coordinated radius (r).

Coordination 14 (IV, VII, IX, XII in P phase; C and E in σ phase): Icositetrahedron with twelve fivefold vertices, represented by one five-coordinated radius (r), and two diametrically opposite sixfold vertices, represented by one six-coordinated radius (r^*); point symmetry D_{6d}.

Coordination 15 (V and X in P phase; B in σ phase): Icosihexahedron with twelve fivefold vertices in two different groups of six, represented by two respective five-coordinated radii (r for the six nearest the trigonal axis, r' for the other six), and three sixfold vertices in the equatorial plane, represented by one six-coordinated radius (r^*); point symmetry D_{3h}.

Coordination 16 (VI in P phase; X and A in α-Mn): Icosioctahedron with twelve fivefold vertices, represented by one five-coordinated radius (r), and four

Table 5. *Ligating radii in P and σ phase*

(All values in Ångström units)

P(Mo–Ni–Cr)					σ(Fe–Cr)		
C.N. 12							
	r				*r*		
I	1·190			*A*	1·161		
II	1·190			*D*(4)	1·169		
III	1·195				1·167		
IV	1·199			A.d.	0·003		
XI(2)	1·188						
	1·192						
A.d.	0·004						
C.N. 14							
	r	*r**			*r*	*r**	
IV	1·447	1·225		*C*	1·395	1·194	
VII	1·436	1·188		*E*	1·376	1·137	
IX	1·442	1·269			1·386	1·166	
XII(2)	1·450	1·188		A.d.	0·010	0·028	
	1·445	1·212					
A.d.	0·005	0·028					
C.N. 15							
	r	*r'*	*r**		*r*	*r'*	*r**
V	1·566	1·509	1·300	*B*	1·498	1·486	1·252
X	1·536	1·564	1·349				
	1·551	1·536	1·324				
A.d.	0·015	0·028	0·024				
C.N. 16							
	r	*r**					
VI	1·613	1·448					

tetrahedrally oriented sixfold vertices, represented by one six-coordinated radius (r^*); point symmetry T_d.

A thirteen-coordinated polyhedron of low symmetry found in α-manganese (D_1) but not in the *P* or σ phases will not be discussed here.

The interesting possibility suggested itself that the atoms in the *P* phase may have radii which conform closely in magnitude to the ideal symmetries of the corresponding polyhedra. On this assumption, the observed interatomic distances were expressed in observational equations as the sums of appropriate pairs of the characteristic radii mentioned above, and the values of these radii (one–three for each atom; twenty-one for twelve different atoms) were determined by the method of least squares. The values obtained are given in Table 5. It will be observed that corresponding radii for similarly coordinated atoms are in remarkable agreement.

As a test of the basic assumption, 'calculated' interatomic distances were obtained by summing the corresponding pairs of atomic radii. For this purpose averages of corresponding radii over similarly coordinated atoms were used, with a resultant reduction of the number of parameters from twenty-one to eight. The resulting 'calculated' distances are compared with the 'observed' distances in Table 4, where it is seen that agreement is remarkably good. Fifty-eight non-equivalent distances, ranging from 2·367 Å to 3·151 Å (a spread of 0·784 Å) are fitted by means of these eight parameters with a weighted mean deviation of 0·035 Å, the largest deviation being 0·122 Å and the next largest 0·093 Å. (The eight parameters could presumably be even reduced to seven, without materially affecting the agreement, by averaging the two kinds of five-coordinated radii on the 15-coordinated atoms V and X.) A parallel calculation was made for the σ phase, using the distances of Bergman & Shoemaker (1954), and the nine radii obtained are listed with the *P*-phase radii in Table 5. These were reduced to six by averaging over similarly coordinated atoms, and 'calculated' interatomic distances were obtained. Agreement with 'observed' distances was almost but not quite as good as in the *P* phase, the average deviation between 'observed' and 'calculated' distances being 0·039 Å. This is an interesting result, in view of the fact that the *P* phase appears to be in some respects a 'distortion' of the σ phase.

By way of contrast, these results may be compared with the results of a more crude previous calculation on the *P* phase in which only one radius value was permitted for each atom. Radii obtained for similarly coordinated atoms were in fairly good agreement, but even when all twelve radii were used in obtaining 'calculated' distances, agreement with 'observed' distances was very unimpressive. The best agreement was for the 12-coordinated atoms, where a mean deviation of 0·050 Å and a maximum deviation of 0·101 Å were obtained. The other atoms showed average deviations grouped closely around 0·12 Å, and maximum deviations as large as 0·395 Å. The overall weighted deviation was 0·096 Å.

Evidently the choice of parameters (in the calculation first described) is a very significant one, and the results obtained have an important bearing on the fundamental nature of the packing and bonding in these structures. The most salient result is that the ligands in these structures divide quite distinctly into two types, namely those described as five-coordinated and those described as six-coordinated. Since the six-coordinated ligands are shorter and therefore presumably stronger with respect to bonding, they may have something of the character of localized covalent bonds, while by comparison the bonding in the five-coordinated ligands may be largely delocalized and more typically metallic. Moreover, the fact that the six-coordinated ligands are found in these structures only in the directionally simple and familiar linear, triangular, and tetrahedral configurations around the central 14-, 15-, and 16-coordinated atoms respectively, suggests that these ligands are bonds formed with some of the various well-known appropriate hybrids, individually or in various possible linear combinations. Presumably the hybrids principally involved are those involving strong participation of *d* orbitals. The five-coordinated radii of the 12-coordinated atoms may correspond uniformly to some mixture of *d*, *s*, and *p* orbitals in approximately the ratio suggested by Pauling (1947) for transition elements, but in the higher-coordinated atoms the *d* character

may be largely preempted by the six-coordinated ligands, resulting in larger radius values.

It is interesting to study the frameworks formed in the σ phase and P phase by these six-coordinated ligands, shown in Fig. 5. These consist of infinite in-

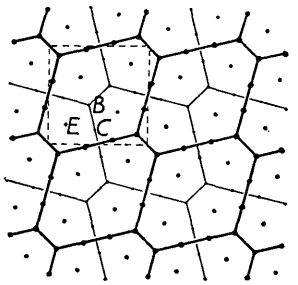

(*a*)

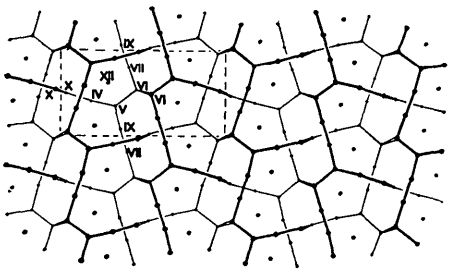

(*b*)

Fig. 5. Frameworks of six-coordinated ligands in (*a*) the σ phase, and (*b*) the P phase. Tapered double lines indicate inclined ligands interconnecting nets on adjacent main layers, and belonging to infinite vertical zigzag rows. Isolated dots indicate infinite straight vertical rows.

dependent vertical chains of 14-coordinated atoms, and of horizontal networks consisting of rows of 14-coordinated atoms with branch points at 15- and 16-coordinated atoms. In the σ phase the horizontal networks (cf. Wells (1956), Fig. 20(*c*), p. 24) are confined to their respective main layers with no interconnections; in the P phase they are interconnected through atoms of kind X and VI into two interlocking but mutually non-interconnected infinite three-dimensional latticeworks.

The excellent general agreement between observed and calculated interatomic distances suggests also that bond numbers corresponding to the various radii tend to be uniform. If we require that both halves of a ligand have the same bond number, this tendency would be propagated throughout the structure, so that all five-coordinated ligands would tend to have a common bond number and all six-coordinated ligands would tend to have a common bond number different from the first. It should be noted that if this tendency is at all strict it would require the valences of the higher-coordinated atoms to be larger than that of the 12-coordinated atoms, since in addition to forming all of the ligands formed by the 12-coordinated atoms the higher-coordinated atoms must form two to four six-coordinated ligands. (The valences calculated from the observed distances by a straightforward application of Pauling's (1947) bond-number equation and single-bond radius values, shown in Table 6, suggest on the contrary that the valence decreases with coordination; similar results were obtained with the σ phase.)

Table 6. *Pauling valences*

C.N. 12		C.N. 14		C.N. 15		C.N. 16	
Atom	Valence	Atom	Valence	Atom	Valence	Atom	Valence
I	6·42	IV	5·20	V	4·71	VI	4·78
II	5·48	VII	5·54	X	5·24		
III	5·81	IX	5·45		4·97		
VIII	5·20	XII	5·54				
XI	6·19		5·43				
	5·82						

Although the scattering parameters are rather rough, the information they provide regarding the distribution of kinds of atoms is in reasonable agreement with indications obtained for the σ phase (Fe–Cr, Bergman & Shoemaker, 1954; Ni–V, Fe–V, and Mn–Cr, Kasper & Waterstrat, 1956). There is no experimental basis for differentiation of nickel and chromium in the P phase, but it is seen that the scattering parameter, and therefore the molybdenum content, increases with the coordination number. The percentage values as given are not normalized (they predict an overall molybdenum content about 5% too high) owing to the choice of limiting values for the scattering parameter. (In the calculation of the Pauling valences given in Table 6 these limiting values were taken somewhat higher (0·80 and 1·37) to obtain approximately normalized molybdenum percentages to be used as weighting factors for single-bond radii.)

It appears plausible on the basis of the present results, and in part by analogy with σ-phase results, that in the P phase the 12-coordinated atoms are mainly nickel, the 14-coordinated atoms mainly mixtures of molybdenum and chromium, and the 15- and 16-coordinated atoms mainly molybdenum.

In the case of the σ phase a strong polyhedron in wave-number space was indicated by the X-ray intensities as corresponding to a Brillouin zone having a capacity of 6·97 electrons per atom with spins paired (Bergman & Shoemaker, 1954), in rather striking accord with the observation of Bloom & Grant (1953) that for binary σ phases, at least in the first long period, the compositions are such that the number of electrons beyond the previous rare-gas shell averages close to seven. In the P phase the corresponding polyhedra is more complicated and not as well defined. Its capacity appears to be closer to 6·5 electrons per atom, while the average number calculated from the composition of the alloy is 7·6. No rational interpretation is apparent at present.

We wish to thank Prof. Paul A. Beck of the University of Illinois for his kindness in donating a specimen of the *P* phase for study, and for much helpful cooperation. Financial support from the Office of Ordnance Research is gratefully acknowledged.

References

ANDREWS, K. W. (1949). *Nature, Lond.* **164**, 1015.
ARNFELT, H. & WESTGREN, A. (1935). *Jernkontor. Ann.* **119**, 185.
BERGMAN, G. & SHOEMAKER, D. P. (1954). *Acta Cryst.* **7**, 857.
BLOOM, D. S. & GRANT, N. J. (1953). *Trans Amer. Inst. Min. (Metall.) Engrs.* **197**, 88.
BRADLEY, A. J. & THEWLIS, J. (1927). *Proc. Roy. Soc.* A, **115**, 456.
BRINK, C. & SHOEMAKER, D. P. (1955). *Acta Cryst.* **8**, 734.
BOOTH, A. D. (1946). *Proc. Roy. Soc.* A, **188**, 77.
DAS, D. K., RIDEOUT, S. P. & BECK, P. A. (1952). *Trans. Amer. Inst. Min. (Metall.) Engrs.* **194**, 1071.
DICKINS, G. J., DOUGLAS, A. M. B. & TAYLOR, W. H. (1951). *Nature, Lond.* **167**, 192.
ELLINGER, F. H. (1942). *Trans. Amer. Soc. Met.* **30**, 607.
GREENFIELD, P. & BECK, P. A. (1954). *Trans. Amer. Inst. Min. (Metall.) Engrs.* **200**, 253, 758.
KASPER, J. S. (1954). *Acta Metallurg.* **2**, 456.
KASPER, J. S., DECKER, B. F. & BELANGER, J. R. (1951). *J. Appl. Phys.* **22**, 361.
KASPER, J. S. & WATERSTRAT, R. M. (1956). *Acta Cryst.* **9**, 289.
PAULING, L. (1947). *J. Amer. Chem. Soc.* **69**, 542.
PAULING, L. (1949). *Proc. Roy. Soc.* A, **196**, 343.
RIDEOUT, S., MANLY, W. D., KAMEN, E. L., LEMENT, B. S. & BECK, P. A. (1951). *Trans. Amer. Inst. Min. (Metall.) Engrs.* **191**, 872.
SHOEMAKER, D. P. & BERGMAN, B. G. (1950). *J. Amer. Chem. Soc.* **72**, 5793.
SHOEMAKER, D. P., BRINK, C. & FOX, A. (1955). Technical Report No. 1, Office of Ordnance Research Project No. 461; also Paper No. 16, Summer 1955 Meeting, American Crystallographic Association, Pasadena, California.
SHOEMAKER, D. P., DONOHUE, J., SCHOMAKER, V. F. H. & COREY, R. B. (1950). *J. Amer. Chem. Soc.* **72**, 2328.
TUCKER, C. W. (1950). *Science*, **112**, 448.
TUCKER, C. W. & SENIO, P. (1953). *Acta Cryst.* **6**, 753.
WELLS, A. F. (1956). *The Third Dimension in Crystallography*. Oxford: Clarendon Press.

Acta Cryst. (1957). **10**, 14

The Prediction of Twinning Modes in Metal Crystals

BY M. A. JASWON AND D. B. DOVE*

Department of Mathematics, Imperial College, London S.W. 7, England

(*Received* 18 *July* 1956)

A new crystallographic analysis of deformation twinning in multiple lattices is developed. This enables the operative twinning modes to be predicted for all metal crystals, including α-uranium. Reasons are given for the non-appearance of certain modes expected theoretically.

Introduction

Deformation twinning of a crystal may be examined from two points of view, the macroscopic and the microscopic. On the macroscopic scale, twinning is achieved by a homogeneous shear parallel to the composition or twinning plane K_1, along a shear direction η_1. The plane perpendicular to K_1, passing through η_1, is termed the plane of shear. Associated with K_1, η_1 there exists a second undistorted plane K_2, cutting K_1 in a direction perpendicular to η_1 and cutting the plane of shear in a direction η_2. Twinned crystals are of two distinct kinds, referred to as first and second. In the former, K_1 is rational, and may be regarded as the plane of an imagined mirror which reflects the structure of the twin into that of the matrix. In the latter, K_1 is irrational, but η_1 is rational, and may be regarded as the direction of an imagined axis about which a rotation of 180° transforms the structure of the twin into that of the matrix. For any given mode

$$K_1 = (hkl),\ K_2 = (h'k'l'),\ \eta_1 = [uvw],\ \eta_2 = [u'v'w'],$$

there exists theoretically a conjugate or reciprocal mode

$$K_1 = (h'k'l'),\ K_2 = (hkl),\ \eta_1 = [u'v'w'],\ \eta_2 = [uvw],$$

involving the same macroscopic shear. From the macroscopic point of view, there should be nothing to choose between a mode and its conjugate, but in certain cases the latter has never been reported operative. The conjugates to the modes (9) and (10), of Table 1, have been reported operative: these are the only established examples in metals of twinning of the second kind.

* Now at Atomic Energy Research Establishment, Harwell, England.